Azetidinimines as a novel series of non-covalent broad-spectrum inhibitors of β-lactamases with submicromolar activities against carbapenemases of classes A, B and D.

Eugénie Romero,[†,#] Saoussen Oueslati,[‡,‖,#] Mohamed Benchekroun,[†,◊] Agathe C. A. D'Hollander,[†,◊] Sandrine Ventre,[†] Kamsana Vijayakumar,[†] Corinne Minard,[†] Cynthia Exilie,[‡,‖] Linda Tlili,[‡,‖] Pascal Retailleau,[†] Agustin Zavala,[†] Eddy Elisée,[†] Edithe Selwa,[†] Laetitia A. Nguyen,[§] Alain Pruvost,[§] Thierry Naas, *[,‡,‖,⊥,¶,◊] Bogdan I. Iorga,*[,†] Robert H. Dodd,[†] Kevin Cariou*[,†,○]

† Université Paris-Saclay, CNRS, Institut de Chimie des Substances Naturelles, LabEx LERMIT, UPR 2301, 91198, Gif-sur-Yvette, France.

‡ UMR1184, Inserm, Université Paris-Saclay, LabEx LERMIT, Hôpital Bicêtre, Le Kremlin-Bicêtre, France.

‖ Bacteriology-Hygiene Unit, Hôpital Bicêtre, Le Kremlin-Bicêtre, France.

§ Université Paris-Saclay, CEA, INRAE, Département Médicaments et Technologies pour la Santé, Gif-sur-Yvette, France.

⊥ EERA Unit "Evolution and Ecology of Resistance to Antibiotics Unit, Institut Pasteur-AP-HP-Université Paris-Saclay, Paris, France.

¶ Associated French National Reference Center for Antibiotic Resistance: Carbapenemase-Producing Enterobacteriaceae, Le Kremlin-Bicêtre, France.

○ Current address: Chimie ParisTech, PSL University, CNRS, Institute of Chemistry for Life and Health Sciences, Laboratory for Inorganic Chemical Biology, 75005 Paris, France.

ABSTRACT

The rise of resistances in Gram negative bacteria is reaching an extremely worrying situation and one of the main causes of resistance is the massive spread of very efficient β-lactamases, which render most β-lactam antibiotics useless. Herein, we report the development of a series of imino-analogs of β-lactams (namely azetidinimines) as efficient non-covalent inhibitors of β-lactamases. Despite the structural and mechanistic differences between serine-β-lactamases KPC-2 and OXA-48 and metallo-betalactamase NDM-1, all three enzymes can be inhibited at a submicromolar level by compound **7dfm**, which can also repotentiate imipenem against a resistant strain of *Escherichia coli* expressing NDM-1. We show that this compound

can efficiently inhibit not only the three main clinically-relevant carbapenemases of Ambler classes A, B and D, but also β-lactamases of all four classes (A, B, C and D). Our results pave the way for the development of a new structurally original family of non-covalent broad-spectrum inhibitors of β-lactamases.

TABLE OF CONTENTS

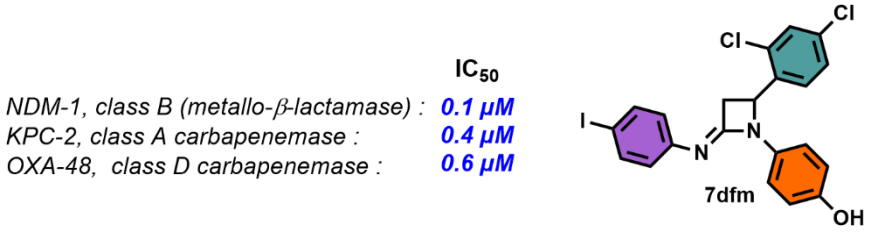

The discovery of penicillin was the start of a golden age for antibiotherapy that is now threatened by exponentially increasing antibioresistance phenomena.[1] Because β-lactams (Figure 1a) have been, and still are, the most prescribed antibiotics worldwide, resistance against them is particularly alarming. Gram negative bacteria (GNB), the main mechanism of β-lactam resistance is due to the production of ß-lactamases, enzymes capable of hydrolyzing β-lactams. Even carbapenems, the most powerful β-lactams, are not spared by metallo-β-lactamases (MBLs) such as NDM-1, IMP-1 or VIM-1 (class B) and/or by some clinically worrisome serine β-lactamases (SBLs) such as KPC-2 or OXA-48 (classes A and D, respectively).[2,3] The discovery of novel antibiotics acting on novel targets is difficult to foresee and strategies to overcome β-lactam resistance[4,5] especially *via* enzyme inhibition[6,7] may preserve our current therapeutic arsenal. This strategy was implemented more than 30 years ago with the development of β-lactamase inhibitors (BLIs) including clavulanic acid or sulbactam (Figure 1b), but was not actively pursued until recently. Since 2012 several new broad-spectrum inhibitors of class A and class C β-lactamases have emerged. Of significant interest, avibactam[8,9] and vaborbactam[10] (Figure 1b) were approved by the FDA for clinical use whilst many of their congeners, in particular diazabicyclooctanes,[11–15] are currently going through preclinical or clinical development. These compounds are mainly able to efficiently inhibit SBLs, including carbapenemases, of class A, C and sometimes D, but generally do not inhibit MBLs (class B). In parallel, continuous efforts for the development of efficient MBL inhibitors[16] have recently led to the identification of promising molecules that can bind to zinc atoms of the active site of MBLs, such as thiols[17] – including the clinically available antihypertensive agent L-captopril[18] –, aspergillomarasmine A,[19] rhodanines[20] and their thienolate derivatives[21] or heteroaryl-carboxylic acids such as ANT431[22] (Figure 1c). Yet there is still no MBL inhibitor available for clinical use. Moreover, the emergence of bacterial isolates

producing two or even three different carbapenemases of different classes now dictates the development of inhibitors capable of simultaneously inhibiting SBLs and MBLs. So far, apart from some polyphenolic derivatives with moderate activities,[23] only boronic acids have been reported to efficiently inhibit both SBLs and MBLs (Figure 1d).

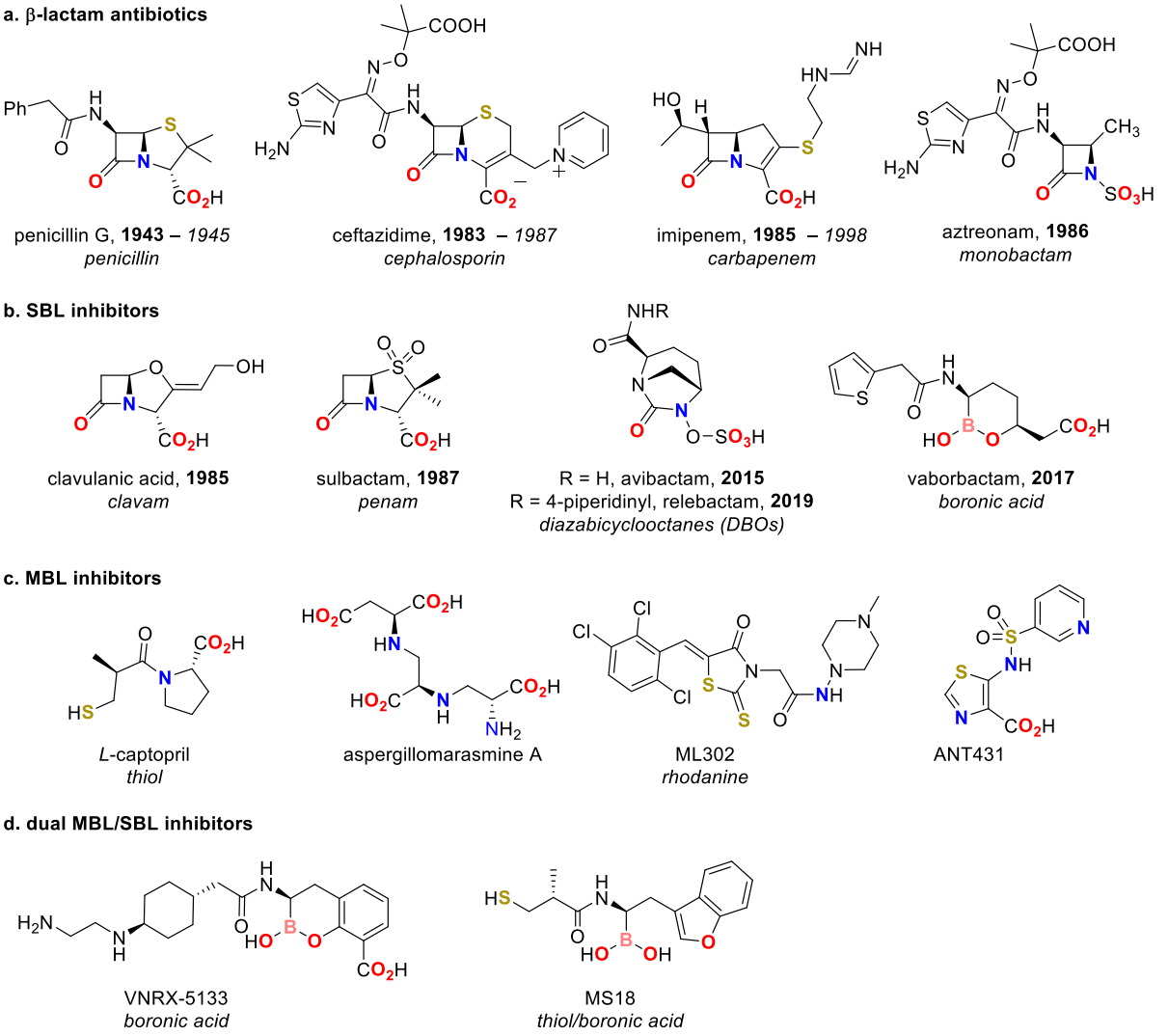

Figure 1. Representative structures of (a) β-lactam antibiotics (in **bold**: year of entry to the market; in *italic*: year of resistance appearance); (b) serine-β-lactamase inhibitors (in **bold**: year of entry to the market); (c) metallo-β-lactamase inhibitors; (d) dual serine-/metallo-β-lactamase inhibitors.

Rigid cyclic analogues of vaborbactam such as VNRX-5133 (currently in phase 3 clinical trials) were the first molecules shown to inhibit all classes of β-lactamases (Figure 1d).[24–27] VNRX-5133 exhibits submicromolar inhibitory activity against most MBLs and SBLs, being only slightly less active against IMP-1 (class B) and OXA-48 (class D). Very recently, thiol/boronic acid hybrids (such as MS18) were developed and demonstrated interesting dual inhibition properties against SBLs and MBLs.[28] MS18 and its congeners also possess a rather broad scope but show limited effects against NDM-1 (class B) and OXA-48.

In this context, we sought to develop novel inhibitors that could block the activities of both SBLs and MBLs with comparable efficiency, specifically targeting the three most clinically-relevant carbapenemases: KPC-2 (class A), NDM-1 (class B) and OXA-48 (class D).

We addressed this challenge by exploring uncharted chemical space around the β-lactam nucleus. Synthetically, this four-membered ring can be obtained by a [2+2] cycloaddition between a ketene and an imine,[29] a reaction named the Staudinger synthesis after its discoverer (Scheme 1a).[30] We recently reported that carefully substituted ynamides[31,32] can be used as precursors for the *in situ* generation of ketenimines[33,34] under mild conditions, which can be intercepted by various heterocyclic nucleophiles[35] or can undergo a microwave assisted [2+2] cycloaddition with imines.[36] By replacing the ketene (C=C=O) with the *in situ* generated iminoketene (C=C=NR), the reaction directly led to an azetidinimine (Scheme 1b). Such imino-β-lactams have only been rarely studied with respect to their synthesis[37,38] and never with respect to their biological and particularly, antibiotic activities. Taking into account their structural similarities with β-lactams, we thus decided to evaluate their therapeutic potential against carbapenemases.

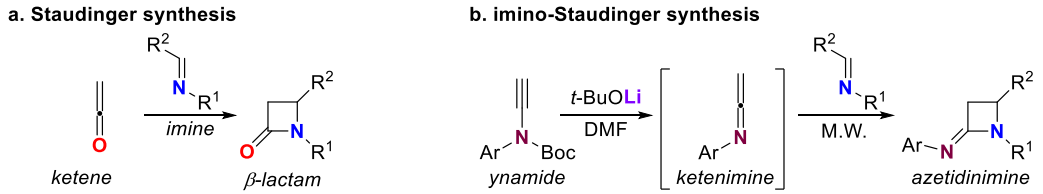

Scheme 1. (a) Staudinger synthesis to access β-lactams; (b) imino-Staudinger synthesis to access azetidinimines.

RESULTS AND DISCUSSION

Chemistry. Taking into consideration the scope and the fact that only aryl groups can be easily incorporated in our previously developed methodology,[36] we devised a convergent synthetic plan to access as many structural variations as possible on the azetidinimine scaffold. The Ar^1 group originated from aniline **1x**, which was protected by a Boc group to give **2x** (Scheme 2). Coupling of **2x** with brominated triisopropylsilylacetylene provided ynamide **3x** after TBAF-promoted desilylation. Condensation of benzaldehyde **4y** with aniline **5z** afforded imines **6yz**.

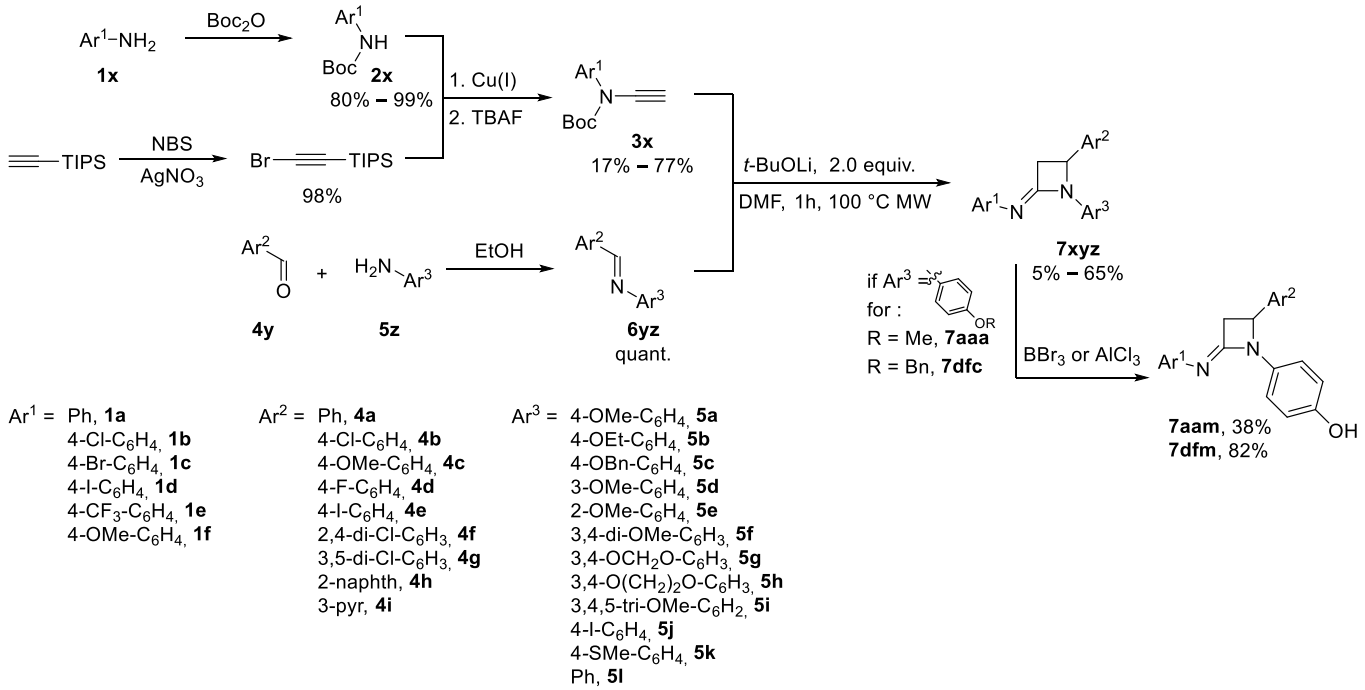

Scheme 2. General synthetic plan to prepare tri-arylated azetidinimines **7xyz**.

The key [2+2] cycloaddition was performed under microwave heating and gave azetidinimines **7xyz** with concomitant loss of the Boc protecting group. For *para*-methoxy derivatives **7aaa**

and **7aba**, as well as *para*-benzyloxy derivative **7dfc**, their corresponding *para*-phenols **7aam**, **7abm** and **7dfm** were obtained by ether cleavage using BBr_3 (for OMe) or $AlCl_3$ (for OBn). More than forty compounds were prepared using this route.

First results. The first compound evaluated was **7aaa**, bearing a *p*-anisyl group on the endocyclic nitrogen. This aryl group was initially chosen for synthetic reasons as it would electronically favor the reaction and could also be easily derivatized. Initial assessment showed that in the presence of 10 µM of **7aaa**, the hydrolysis of imipenem by NDM-1 was inhibited by 90% with an IC_{50} estimated to be between 2 and 5 µM (Table 1). This very encouraging initial result prompted us to try and rationalize this inhibitory activity by performing *in silico* molecular modeling studies (Figure 2). It appeared that the azetidinimine does not behave like a β-lactam, whose carbonyl group is chelated by the zinc ions during the hydrolysis process. Here, the methoxy group is coordinated by both zinc ions in the active site and the four-membered ring acts as a scaffold to position the two phenyl rings in hydrophobic regions of the enzyme active site. The Ar^1 phenyl substituent is surrounded by Ser251, Asp212, Ala 215 and Ser217 for both enantiomers, whereas the Ar^2 phenyl substituent is positioned near Asn220 in the *R* enantiomer and in the proximity of Val73, Ile 35, Met67 and Phe70 in the *S* enantiomer (Figure 2). The two enantiomers of **7aaa** were separated by chiral chromatography and then tested separately, both showing similar inhibition of NDM-1.

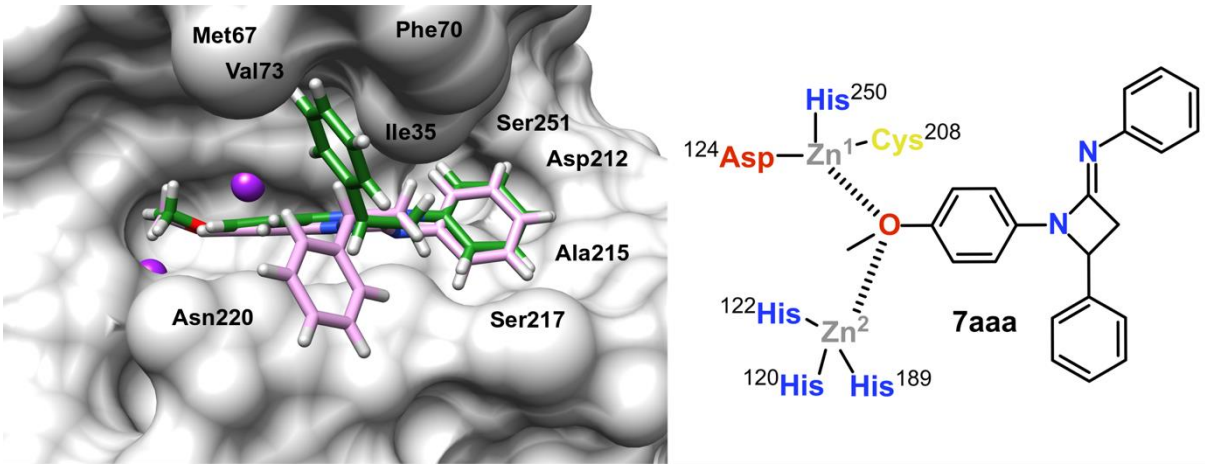

Figure 2. Docking of compound **7aaa** in the active site of NDM-1 (left) and schematic drawing of its key interactions with the zinc ions (right). The enantiomers *R* and *S* of **7aaa** are colored in pink and green, respectively, and the zinc ions are colored in purple.

SAR for enzyme inhibitory activities. A systematic structure-activity relationship was then undertaken by varying the aromatic groups around the azetidinimine nucleus and targeting three carbapenemases: NDM-1, OXA-48 and KPC-2. In addition to its NDM-1 inhibitory activity, **7aaa** was found to be moderately active against KPC-2 but did not have any activity against OXA-48 (Table 1). Variations of the Ar^3 ring showed that minimal modifications such as replacing the methoxy of **7aaa** by an ethoxy (**7aab**) or a benzyloxy (**7aac**) led to an improvement of the activity against all three enzymes, **7aac** in particular displaying a sub-micromolar activity against NDM-1 (0.4 µM). Similar activities to **7aab** and **7aac** were observed when the methoxy group was in the meta position (**7aad**). However, the presence of two methoxy groups (**7aaf**), or a benzo[d][1,3]dioxole moiety (**7aag**), led to a slight decrease of efficiency against NDM-1 and a loss of activity for OXA-48 and KPC-2. This was partially restored by incorporation of a 2,3-dihydrobenzo[b][1,4]dioxane, as **7aah** was found to be quite similar to **7aad** in terms of inhibition profile. While 3,4,5-trimethoxy derivative **7aai** only maintained a low activity for NDM-1, aniline-derived compound **7aaj** was found to inhibit all three enzymes with IC_{50}'s of 10.0, 7.0 and 3.5 µM, respectively. The incorporation of an iodine atom (**7aak**) on the *para* position led to solubility issues preventing data from being obtained against OXA-48 and KPC-2 although the anti NDM-1 activity could nevertheless be evaluated to be in the 4.0-5.0 µM range. The thiomethyl derivative **7aal** was also poorly soluble in water, but its strong affinity for the active site Zn ions led to a high inhibition of NDM-1. Finally, the free phenol **7aam** was moderately active against KPC-2 and OXA-48 but again exhibited high inhibitory properties against NDM-1 (0.8 µM). To conclude in this series of Ar^3 variations, the best *pan*-carbapenemase inhibitors were *p*-oxyphenyl compounds and especially those bearing a benzyloxy (**7aac**) and a free hydroxy (**7aam**).

Table 1. Influence of Ar^3 on NDM-1, OXA-48 and KPC-2 inhibitory activities compared to **7aaa**.

Compound	**IC_{50} (µM) or** *% inhibition*		
	NDM-1	**OXA-48**	**KPC-2**
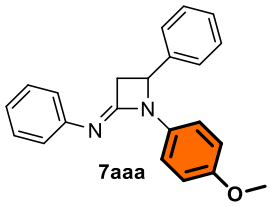 **7aaa**	2.0–5.0	N.E.	*55% inhibition at 10 µM*
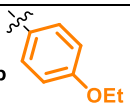 **7aab**	2.0–5.0	*45% inhibition at 10 µM*	2.0–5.0
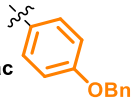 **7aac**	**0.4**	*31% inhibition at 10 µM*	**1.6**
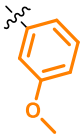 **7aad**	**1.3**	*28% inhibition at 10 µM*	5.0–10.0
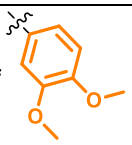 **7aaf**	5.0–10.0	*9% inhibition at 10 µM*	*17% inhibition at 10 µM*
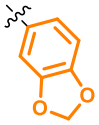 **7aag**	5.0	*20% inhibition at 10 µM*	*6% inhibition at 10 µM*
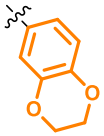 **7aah**	**1.6**	*37% inhibition at 10 µM*	5.0–10.0
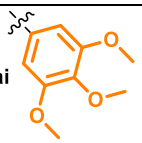 **7aai**	*78% inhibition at 50 µM*	N.E.	N.E.
 **7aaj**	10.0	7.0	3.5
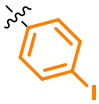 **7aak**	4.0–5	N.D.	N.D.
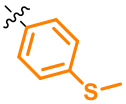 **7aal**	**<1.0**	*15% inhibition at 10 µM*	*82% inhibition at 20 µM*
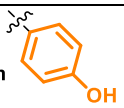 **7aam**	**0.8**	*26% inhibition at 10 µM*	*45% inhibition at 10 µM*

N.E.: no effect (at 10 µM); N. D.: not determined

Keeping a *para*-methoxyphenyl group as Ar^3, variations of Ar^2 were then examined for activity and compared to **7aaa** (Table 2). The *p*-chloro analogue (**7aba**) maintained a similar activity against NDM-1 and though some anti-OXA-48 activity was witnessed, its anti-KPC-2 effect was largely lost. Both *p*-methoxy and *p*-fluoro analogues **7aca** and **7ada** were rather inefficient on all three enzymes while the *p*-iodo, 3,5-dichloro and 2-naphthyl derivatives (**7aea**, **7aga** and **7aha** respectively) presented an interesting profile, being almost equipotent against NDM-1 and KPC-2 but somewhat less effective against OXA-48. In contrast, pyridinyl compound **7aia** was almost inactive on all three enzymes.

Table 2. Influence of Ar^2 on NDM-1, OXA-48 and KPC-2 inhibitory activities compared to **7aaa**.

Compound	**IC_{50} (µM) or** *% inhibition*		
	NDM-1	**OXA-48**	**KPC-2**
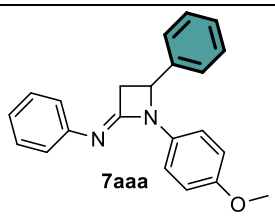 **7aaa**	2.0–5.0	N.E.	*55% inhibition at 10 µM*
7aba 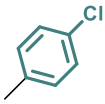	2.0–5.0	*21% inhibition at 50 µM*	*44% inhibition at 50 µM*
7aca 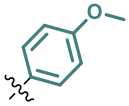	*67% inhibition at 10 µM*	*3% inhibition at 10 µM*	*7% inhibition at 10 µM*
7ada 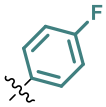	*9% inhibition at 10 µM*	N.D.	*10% inhibition at 10 µM*
7aea 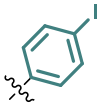	**1.1**	*33% inhibition at 10 µM*	**1.1**
7aga 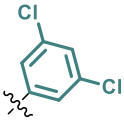	2.0–5.0	*15% inhibition at 5 µM*	2.0–5.0
7aha 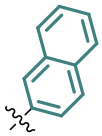	2.0–5.0	10.0-20.0	5.0-7.0
7aia 	*23% inhibition at 100 µM*	N.E.	*12% inhibition at 100 µM*

N.E.: no effect (at 10 µM); N. D.: not determined

From these results, two Ar^2 groups were selected: *para*-chloro and 2-naphthyl (as in **7aba** and **7aha**). At this stage, we wished to evaluate the influence of Ar^1in both series (4-chloro in Table 3 and 2-naphthyl in Table 4). It is worth noting that 4-chloro derivatives generally exhibit a greater ease of synthesis due to the superior reactivity of imine **6bz** (or **6fz**) in the [2+2] cycloaddition. Compared to **7aba**, the introduction of a substituent at the *para* position of Ar^1 – whether a chloro (**7bba**), a bromo (**7cba**), an iodo (**7dba**), a trifluoromethyl (**7eba**) and to a lesser extent a methoxy group (**7fba**) – was highly beneficial for the anti-NDM-1 activity, with all compounds possessing IC_{50} values in the 0.5-0.8 µM range (Table 3).

Table 3. Influence of Ar^1 on NDM-1, OXA-48 and KPC-2 inhibitory activities compared to **7aba** and **7cfa**.

Compound	**IC_{50} (µM) or** *% inhibition*		
	NDM-1	**OXA-48**	**KPC-2**
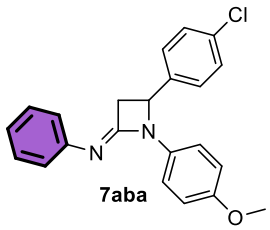 **7aba**	2.0–5.0	*21% inhibition at 50 µM*	*44% inhibition at 50 µM*
7bba 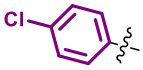	**0.5**	*27% inhibition at 10 µM*	2.9
7cba 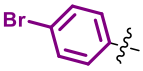	**0.6**	7.6	2.4
7dba 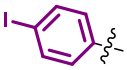	**0.7**	7.5	2.7
7eba 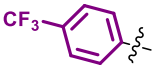	**0.7**	*32% inhibition at 10 µM*	3.6
7fba 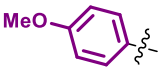	**1.9**	*31% inhibition at 10 µM*	N.E.
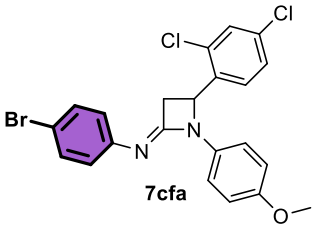 **7cfa**	**1.2**	*46% inhibition at 10 µM*	*30% inhibition at 10 µM*
7dfa 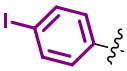	**0.5**	8.5	2.9
7efa 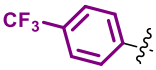	**0.8**	5.9	8.7

N.E.: no effect (at 10 µM)

The IC_{50}'s against KPC-2 were also improved with values between 2.0 and 3.6 µM, except for (**7fba**). Additionally, the IC_{50}'s against OXA-48 dropped under the 10 µM threshold for two compounds (**7cba** and **7dba**). A similar trend could be observed with an additional chloro at the 2 position of Ar^2 (2,4-dichloro series): the *para*-iodo (**7dfa**) and *para*-trifluoromethyl (**7efa**) were found to be the most potent *pan*-inhibitors of carbapenemases NDM-1, OXA-48 and KPC-2 in this series.

Table 4. Influence of Ar^1 on NDM-1, OXA-48 and KPC-2 inhibitory activities compared to **7aha** and **7ahb**.

Compound	**IC_{50} (µM) or** *% inhibition*		
	NDM-1	**OXA-48**	**KPC-2**
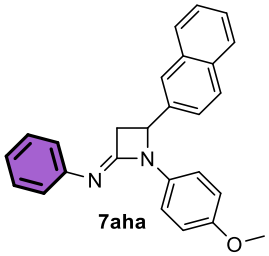 **7aha**	2.0–5.0	10.0-20.0	5.0-7.0
7bha 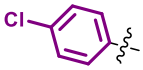	**1.6**	*18% inhibition at 10 µM*	5.7
7cha 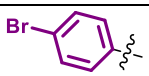	**1.1**	3.6	7.5
7dha 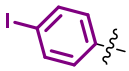	**0.5**	7.6	2.3
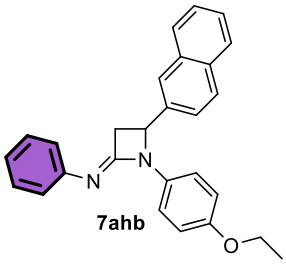 **7ahb**	5.0–7.0	N.D.	N.D.
7bhb 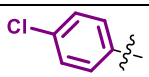	**0.6**	*30% inhibition at 10 µM*	2.8
7dhb 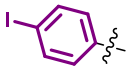	**0.5**	6.2	2.5
7fhb 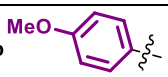	**0.6**	7.4	2.4

N. D.: not determined

Similarly, excellent anti-NDM-1 activities were observed in the Ar^2 = naphthyl series (Table 4), with four compounds (**7dha**, **7bhb**, **7dhb** and **7fhb**) having submicromolar IC_{50}'s. Activities against KPC-2 and OXA-48 were also significantly improved, being always under 10 µM except in the case of *para*-chlorinated derivatives **7bha** and **7bhb** (for OXA-48). Despite their high activity, the increased lipophilicity brought by the naphthyl group (for **7dhb** $logP_{theor}$ = 6.94) caused products in this series to be very poorly soluble and to easily form aggregates in the assay media. Thus further studies within this series were stopped.

Having witnessed the highly favorable effect of the *para* substitution on Ar^1 and keeping in mind the importance of the *para*-alkoxy moiety on Ar^3, further study of the influence of Ar^2 was carried out with **7dba** as reference (Table 5). All compounds in this series offered a rather broad-spectrum of activity with most of them inhibiting all carbapenemases with an IC_{50} below 10 µM and even submicromolar for NDM-1. In contrast with the other compounds, *p*-fluoro (**7dda**), *p*-iodo (**7dea**) and 3,5-dichloro (**7dga**) analogues were more active against OXA-48 than against KPC-2. Finally, keeping Ar^1 = *p*-iodophenyl and Ar^2 = 2,4-dichlorophenyl (**7dfa**), variations on Ar^3 were then further investigated. Surprisingly (compared with **7aaa** and **7aac** in Table 1), the *p*-benzyloxyphenyl derivative (**7dfc**) proved to be less active than **7dfa** (Table 5). **7dfc** was then converted into a free phenol (**7dfm**) by $AlCl_3$-mediated cleavage of the ether bond (see Scheme 3). This compound exhibited submicromolar IC_{50} activity against the three enzymes: 0.1 µM for NDM-1 (which could be explained by stronger interactions of the OH function with the zinc ions of the active site), 0.4 µM for OXA-48 and 0.6 µM for KPC-2. While the homologous benzylic alcohol analogue **7dfn** was found to be less active, the corresponding carboxylic acid **7dfo** (obtained by oxidation of **7dfn** with $KMnO_4$, see Scheme 3) was the most active compound on NDM-1 so far (0.07 µM) but with a complete loss of activity against OXA-48.

Table 5. Influence of Ar^2 compared to **7dba** and of Ar^3compared to **7dfa** on NDM-1, OXA-48 and KPC-2 inhibitory activities

Compound	IC_{50} (µM)		
	NDM-1	**OXA-48**	**KPC-2**
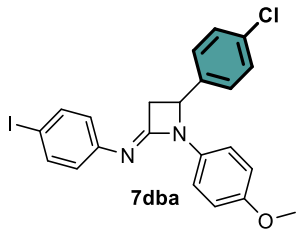 **7dba**	**0.7**	7.5	2.7
7dda 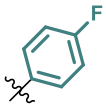	**1.0**	4.2	9.5
7dea 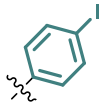	**0.7**	4.4	8.5
7dha 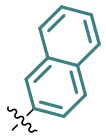	**0.5**	7.6	2.3
7dga 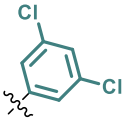	4.5	4.8	*42% inhibition at 10 µM*
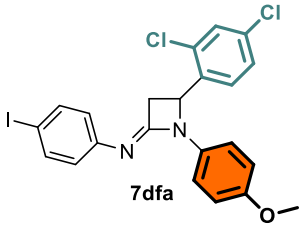 **7dfa**	**0.5**	8.5	2.9
7dfc 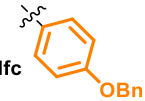	**0.8**	*41% inhibition at 10 µM*	5.5
7dfm 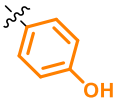	**0.1**	**0.4**	**0.6**
7dfn 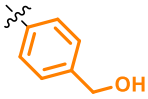	3.0	N.E.	6.0
7dfo 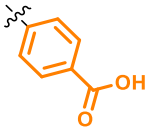	**0.07**	N.E.	6.0

N.E.: no effect (at 10 µM); N. D.: not determined

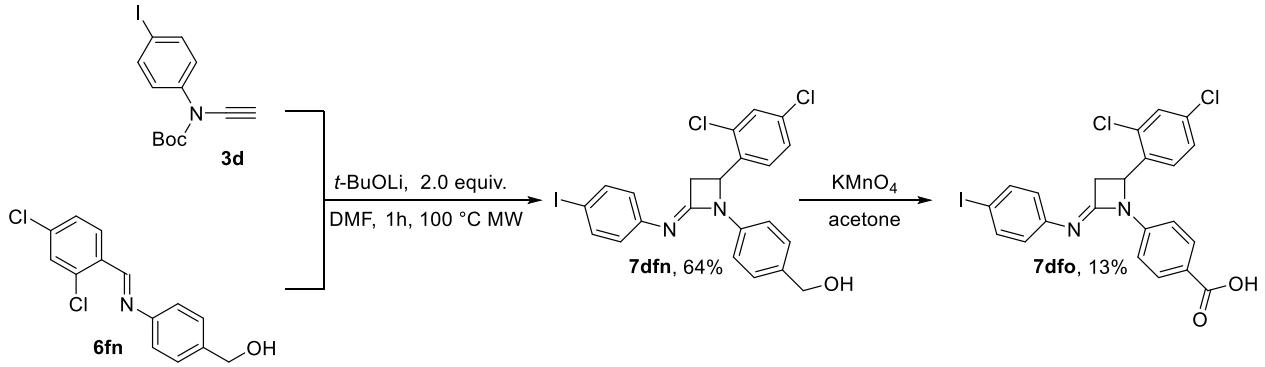

Scheme 3. Synthesis of compounds **7dfn** and **7dfo**.

Complementary assays. Having found a lead (**7dfm**) in our novel azetidinimine BLI series, we then performed complementary assays to ascertain its therapeutic potential. First, it was screened at 10 µM against a wider panel of BLs (Table 6). At this concentration a complete inhibition of three NDM variants (NDM-4, NDM-7 and NDM-9) and of VIM-1 (Class B) was observed. In contrast, VIM-52 (class B) was not affected. The extended-spectrum β-lactamase CTX-M-15 (class A) and the cephalosporinase CMY-2 (class C) were also inhibited (83% and 86%, at 10 µM, respectively). These latter results demonstrate that compound **7dfm** can inhibit not only *carbapenemases from 3 classes* but, more generally, ***BLs from all four classes***.

Table 6. Additional enzymatic inhibitory activities (% at 10 µM) for **7dfm**

Compound	NDM-4	NDM-7	NDM-9	VIM-1	VIM-52	CTX-M-15	CMY-2
7dfm	**100%**	**100%**	**100%**	**100%**	0%	83%	86%

The metabolic stability of **7dfm** was evaluated and the compound was found to possess an excellent stability profile with a Cl_{int} of µL/min/mg protein in mouse hepatic cells (Table 7). The toxicity of **7dfm** was measured against both normal cells (MRC-5) and cancer cells (HCT-116) and was found to be in the 20-30 µM range, that is, almost two orders of magnitude higher than its IC_{50} against carbapenemases. Finally, compound **7dfm** was evaluated for the repotentiation of imipenem against the clinical strain of *E. coli* that expresses NDM-1 (amongst other genes of resistance).[39] In the absence of inhibitor the MIC was above the resistance

threshold at 16 µg/mL, in the presence of 20 µM of **7dfm** it was divided by 2, while using 50 µM of **7dfm** it was divided by 4, bringing it down to the intermediate/resistant limit.

Table 7. Metabolic stability, cytotoxicity and imipenem repotentiation for **7dfm**

	Stability		**IC_{50} (µM)[c]**		**MIC (µg/mL)[d]**		
	Non-NADPH[a]	CL_{int}[b]	MRC-5	HCT-116	0µM	20µM	50µM
7dfm	**96%**	**13.9**	19.9	32.3	16	8	**4**

[a] Stability after 45 min in the presence of mouse hepatic microsome in the absence of NADPH; [b] CL_{int} was determined using mouse hepatic microsomes and is given in µL/min/mg protein; [c] inhibition of cell proliferation; [d] Minimum inhibitory concentration for imipenem using *E. coli* GUE-NDM1[39] clinical strain.

Molecular modeling Compound **7dfm** was selected for a more in depth study of the interaction with the three main clinically-relevant carbapenemases, NDM-1, KPC-2 and OXA-48. The docking of these three enzymes with the two enantiomers of **7dfm** was performed using GOLD[40] and the results are presented in Figure 4.

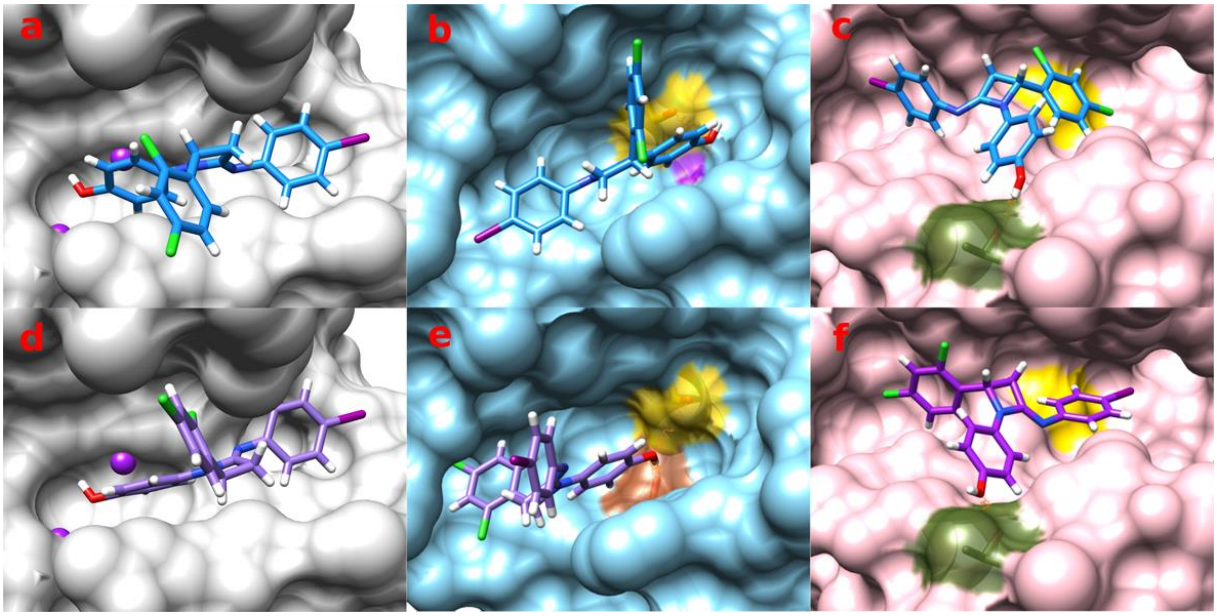

Figure 4: Docking conformations of the enantiomers *R* (**a**, **b**, **c**) and *S* (**d**, **e**, **f**) of compound **7dfm**, in the active site of NDM-1 (class B) represented as gray surface (**a**, **d**), KPC-2 (class A) represented as light blue surface (**b**, **e**) and OXA-48 (class D) represented as pink surface (**c**, **f**). For NDM-1, the zinc ions are colored in purple, for KPC-2 the residues Ser70, Lys73 and Ser130 are colored in yellow, purple and brown, respectively, and for OXA-48 the residues Ser70 and Thr104 are colored in yellow and olive, respectively. Hydrogen bonds are represented as springs colored in orange.

With NDM-1, both enantiomers of **7dfm** interact in a similar manner as **7aaa** (see Figure 2). The phenol moiety is coordinated with the two zinc ions and the 4-iodo-phenyl substituent is positioned in the same subpocket in both cases, possibly establishing a stabilizing halogen bond with the side chain of Asp212. The 2,4-dichloro-phenyl substituent is positioned in a hydrophobic environment bordered by residues Val73, Ile35, Met67 and Phe70 for the *S* enantiomer (Figure 4d) and in the vicinity of Asn220 for the *R* enantiomer (Figure 4a).

The docking pose of KPC-2 with the *R* enantiomer (Figure 4b) shows two hydrogen bonds between the phenol group of **7dfm** and the side chains of Ser70 and Lys73. The 4-iodo-phenyl substituent is positioned in a subpocket formed by the side chains of Asn218, His219 and Glu276 and may form a halogen bond with the side chain of Asn218, whereas the 2,4-dichloro-phenyl substituent is more solvent exposed. The *S* enantiomer makes hydrogen bonds with the side chains of Ser70 and Ser130 through the phenol substituent (Figure 4e), and the positions of the other two substituents are inverted compared with the *R* enantiomer.

The interaction of OXA-48 with the *R* enantiomer of **7dfm** (Figure 4c) shows a hydrogen bond between the phenol group and the side chain of Thr104, at the upper extremity of the binding site, whereas the two other substituents are positioned more deeply in the binding site groove. The *S* enantiomer establishes the same hydrogen bond between the phenol group and the side chain of Thr104, with the positions of the 4-iodo-phenyl and 2,4-dichloro-phenyl substituents inverted.

Conclusions

The evaluation of azetidinimines, imino-analogues of β-lactams, as β-lactamase inhibitors led to the development of a new family of non-covalent carbapenemase inhibitors. Structural

optimization led to the identification of phenol **7dfm** as the lead compound, which can strongly inhibit MBL NDM-1 (0.1 µM), class A SBL KPC-2 (0.4 µM), and class D SBL OXA-48 (0.6 µM). Molecular modeling showed that this compound does not mimic a β-lactam within the enzyme active sites and that both enantiomers can interact with the enzymes. Provided one key interaction (such as complexation with the zinc ions in NDM-1 or hydrogen bonds in KPC-2 and OXA-48) is established, the rigid and compact structure of the central four-membered ring indeed allows the other aryl groups to be allocated almost interchangeably in the enzyme pocket to increase the affinity. Further refinement of the structure of these molecules will be pursued to improve the efficiency of these β-lactamase *pan* inhibitors. The metabolic stability of the hit compound and its efficient repotentiation of imipenem against a resistant *E. coli* strain will serve as the basis for future *in vivo* studies.

Materials and Methods

General Procedure for Azetidinimine Synthesis. The imine (1.0 equiv.), the ynamide (2.0 equiv.) and the additive – silica gel (1.0 equiv.) or $ZnOTf_2$ (10 mol%) – were successively added in a microwave sealable tube and placed under argon before the addition of *t*-BuOLi – solid or 2.2 M in solution in THF – (2.0 equiv.) followed by extra dry DMF (0.3M). The sealed tube was placed in a microwave apparatus for 1 h at 100 °C. The crude material was purified by flash chromatography on silica gel or with preparative TLC. See Supporting Information for detailed synthetic procedures and characterizations of the compounds.

***In vitro* β-lactamase inhibition assay.** IC_{50} values were determined against the panel of purified carbapenemases: OXA-48, KPC-2 and NDM-1 by spectrophotometric assay, using ULTROSPEC 2000 UV spectrophotometer and the SWIFT II software (GE Healthcare, Velizy-

Villacoublay, France). Compounds were dissolved in DMSO stock solutions at 10 mM; more dilute stocks were subsequently prepared as necessary by dissolving them also in DMSO. Assay conditions were as follows: 100 mM phosphate buffer, pH 7 (supplemented with 50 µM Zn^{2+} when testing NDM-1, and with 50 mM $NaHCO_3$ when testing OXA-48), 100 µM imipenem (Sigma-aldrich, Saint-Quentin Fallavier, France). The reaction was monitored at 297 nm, time course 600 seconds at 25°C with 3 min of incubation (compound/carbapenemase). Each inhibitor compound was assayed at seven different concentrations, in triplicate for calculating an error value with 95% confidence interval ($\rho < 0.05$). IC_{50} values were determined using the equation $IC_{50} = ((1/0.5 \times v0) - m)/q$, where v0 is the rate of hydrolysis of the reporter substrate (v0 being the rate measured in the absence of inhibitor), q the y axis intercept and m the slope of the resulting linear regression. Percentage of inhibition were obtained with a concentration of 10 µM of compound.

Minimal Inhibition concentrations. MIC values were determined by broth microdilution, in triplicate, in cation-adjusted Mueller Hinton broth according to the Clinical Laboratory Standards Institute (CLSI, https://clsi.org/) guidelines. The enterobacterial clinical strain *E. coli* NDM-1 GUE expressing the carbapenemase NDM-1 was used.[39] Experiments were performed in microtiter plates containing the medium with imipenem and inhibitors (dissolved in DMSO). Three inhibitor concentrations were tested: 50, 100 and 200 µM. Plates were incubated overnight at 37°C for 18−24 h.

Incubations in hepatic microsomes. Compounds (5 µM) were incubated in 0.5 mg/mL of pooled male mouse liver microsomes (from Biopredic, France), in 0.1 M phosphate buffer at pH 7.4 at 37 °C. After prewarming the mixture for 5 min, reactions were initiated by the addition of NADPH (1 mM). Incubations (400 µL) were performed at 37 °C for 0, 5, 15, 30 and

45 min in duplicate and the reaction immediately terminated by adding 200 µL of cold acetonitrile. Samples (including the control to evaluate non NADPH-dependent stability) were centrifuged and the supernatant fractions analyzed by UPLC-MS/MS with multiple reaction monitoring (MRM). Diphenhydramine was used as positive control in mouse liver microsomes test. The MRM area response of the analyte was set to 100% with the T0 incubation, the relative decrease in MRM area ratio intensity over time against that of the control (percent parent decrease) was used to determine the half-life (t1/2) of compounds in the incubation. Half-life values were calculated from the relationship:

T1/2 (min) = 0.693/k, where k is the slope of the Ln concentration vs time curve. The intrinsic clearance (CLint) was calculated as: CLint = (0.693 x incubation volume (µL))/(t (min) x mg of microsomal protein).

Cell culture and proliferation assay. Assays were carried out at the Institut de Chimie des Substances Naturelles by the CIBI screening platform. Cell lines were obtained from the American type Culture Collection (Rockville, USA) and were cultured according to the supplier's instructions. Briefly, human MRC-5 cells were grown in DMEM supplemented with 10% fetal calf serum (FCS) and 1% glutamine and HCT116 colorectal carcinoma cells were grown in RPMI 1640 containing 10% FCS and 1% glutamine. All cell lines were maintained at 37 °C in a humidified atmosphere containing 5% CO_2. Cell growth inhibition was determined by an MTS assay according to the manufacturer's instructions (Promega, Madison, WI, USA). Briefly, the cells were seeded in 96-well plates (2.5 × 103 cells/well) containing 200 µL of growth medium. After 24 h of culture, the cells were treated with the test compounds at different final concentrations. After 72 h of incubation, 40 µL of resazurin was added for 2 h before recording absorbance at 490 nm with a spectrophotometric plate reader. The IC_{50} value

corresponded to the concentration of compound inducing a decrease of 50% in absorbance of drug-treated cells compared with untreated cells. Experiments were performed in triplicate. Paclitaxel was used as the reference compound.

PCR, Cloning, Expression, and DNA Sequencing. Whole-cell DNA of the enterobacterales expressing β-lactamases NDM-1, NDM-4, NDM-7, NDM-9, VIM-1, VIM-52, CTX-M-15, CMY-2 and OXA-48 was extracted, using the QIAamp DNA mini kit (Qiagen, Courtaboeuf, France) and used as a template to amplify all the different genes. The sequences without the peptide signal (predicted by SignalIP 4.1 Server, http://www.cbs.dtu.dk/services/SignalP-4.1/) encoding for the mature protein, were obtained by PCR amplification, using the forward primers, which included an *Nde*I restriction site, and the reverse primer which included an *Xho*I restriction site and a deletion of the stop codon of the gene to allow the expression of an C_Term His tag. Then, PCR product was cloned into pET41b vector (Invitrogen®, Life Technologies, Cergy-Pontoise, France), using *Nde*I and *Xho*I restriction enzymes, to obtain a C-Term His_8-tag. The accuracy of the recombinant plasmid was verified by sequencing, using a T7 promoter and T7 terminator with an ABI Prism 3100 automated sequencer (Applied Biosystems, Thermo Fisher Scientific, Les Ulis, France). The nucleotide sequences were analyzed by using software available at the National Center for Biotechnology Information website (http://www.ncbi.nlm.nih.gov).

Protein purification. An overnight culture of *E. coli* BL21 DE3 harboring recombinant pET41b plasmids was used to inoculate 2 L of LB medium broth containing 50mg/L kanamycin. Bacteria were cultured at 37 °C until an OD of 0.6 at 600 nm was reached. The expression of the β-lactamase genes was carried out overnight at 22 °C with 0.2 mM IPTG as inducer. Cultures were centrifuged at 6000 g for 15 min and then the pellets were resuspended with the binding

buffer (10 mM imidazole, 25 mM sodium phosphate pH 7.4 and 300 mM NaCl). Bacterial cells were disrupted by sonication and the bacterial pellet was removed by two consecutive centrifugation steps at 10000g for 1h at 4 °C; the supernatant was then centrifuged at 96000g for 1h at 4 C. The soluble fractions were filtered and then passed through a HisTrapTM HP column (GE Healthcare) and proteins were eluted with the elution buffer (500 mM imidazole, 25 mM sodium phosphate pH 7.4 and 300 mM NaCl). Finally, a gel filtration step was performed with 100 mM sodium phosphate buffer pH 7 and 150 mM NaCl with a Superdex 75 column (GE Healthcare). The protein purity was estimated by SDS–PAGE. The pooled fractions were dialyzed against 10 mM Tris-HCl pH 7.6, for NDM and VIM 50 µM of $ZnSO_4$ was added, then concentrated using Vivaspin columns (Sartorius, Aubagne, France). The concentrations were determined by measuring the OD at 280 nm and with the extinction coefficients obtained from the ProtParam tool (Swiss Institute of Bioinformatics online resource portal).[41]

Molecular modeling. The three-dimensional structure of compound **7aaa**[36] was retrieved from the Cambridge Structural Database[42] (CSD refcode KEMJEU) and that of compound **7dfm** were built starting from **7aaa** by manual editing using UCSF Chimera package.[43] The structures of enantiomers were generated using an in-house script. Molecular docking was performed using the GOLD suite[40] (CCDC) and the GoldScore scoring function, with the structures 4HL2,[44] 2OV5[45] and 4S2P[46] as receptors for NDM-1, KPC-2 and OXA-48, respectively. The binding sites were defined as 15 Å radius spheres centered on the Zn1 ion for NDM-1 and on the OG atom of Ser70 for KPC-2 and OXA-48. In agreement with our previous studies[47–53] showing that an enhanced conformational search is beneficial, especially for large molecules, a search efficiency of 200% was used to better explore the ligand conformational space. All other parameters were used with the default values. Images were generated using UCSF Chimera.[43]

Supporting Information

The Supporting Information contains detailed synthetic procedures and characterizations of the compounds and copies of the NMR spectra.

Author Information

Corresponding authors:

*E-mail: kevin.cariou@cnrs.fr

*E-mail:bogdan.iorga@cnrs.fr.

*E-mail:thierry.naas@aphp.fr.

ORCID:

Alain Pruvost: 0000-0002-7781-7735

Thierry Naas: 0000-0001-9937-9572

Bogdan I. Iorga: 0000-0003-0392-1350

Kevin Cariou: 0000-0002-5854-9632

Author Contributions

This study was conceived by K. Cariou, B. I. Iorga, T. Naas and R. H. Dodd. Synthesis and characterization of the compounds were performed by E. Romero, M. Benchekroun, S. Ventre, A. C. A. D'Hollander, K. Vijayakumar and C. Minard. Purification of the proteins, inhibition assays and MIC assays were performed by S. Oueslati with C. Exilie, L. Tlili and A. Zavala. Metabolic studies were performed by L. A. Nguyen under the supervision of A. Pruvost. Structural analysis and molecular modeling studies were performed by A. Zavala, E. Elisée, E.

Selwa, P. Retailleau and B. I. Iorga. K. Cariou and B. I. Iorga drafted the manuscript which was amended and commented on by all authors.

# E. R. & S. O contributed equally; ◊ M. B. & A. C. A. D. contributed equally

.

Conflict of Interest Disclosure: The authors declare no competing financial interest

List of Abbreviations

CTX M 15: Cefotaximase-Munich 15

CMY-2: Cephamycinase-2

DMSO: dimethyl sulfoxideGNB: Gram-negative Bacilli

HCT 116: Human Colorectal Carcinoma cells

KPC: Klebsiella Pneumoniae Carbapenemase

MBL: Metallo-β-lactamase

MIC: Minimum Inhibitory Concentrations

MRC-5: Medical Research Council cell strain 5

ND: Not Determined

NDM: New Delhi metallo-β-lactamase

NE: no effect

OXA: Oxacillinase

SAR: Structure Activity Relationship

SBL: Serine-β-lactamases

VIM: Verona Integron metallo-β-lactamase

Acknowledgments

This work was supported by the Laboratory of Excellence in Research on Medication and Innovative Therapeutics (LERMIT, grant ANR-10-LABX-33 under the program Investissements d'Avenir ANR-11-IDEX-0003-01), the FCS Campus Paris-Saclay pre-maturation program (project Inhibase), the SATT Paris-Saclay (project CARBAMAT), the JPIAMR transnational project DesInMBL (grant ANR-14-JAMR-0002) and the Région Ile-de-France (DIM Malinf). The authors also thank CNRS, AP-HP, Université Paris-Saclay, and ICSN, for financial support.

References

1. O'Neill, J. (2016). *Tackling drug-resistant infections globally: final report and recommendations. https://amr-review.org/sites/default/files/160525_Final%20paper_with%20cover.pdf*.

2. Nordmann, P., Naas, T., Fortineau, N. and Poirel, L. (2007). Superbugs in the coming new decade; multidrug resistance and prospects for treatment of Staphylococcus aureus, Enterococcus spp. and Pseudomonas aeruginosa in 2010. *Curr. Opin. Microbiol. 10*, 436–440.

3. Nordmann, P., Naas, T. and Poirel, L. (2011). Global spread of carbapenemase-producing enterobacteriaceae. *Emerg. Infect. Dis. 17*, 1791–1798.

4. Worthington, R. J. and Melander, C. (2013). Overcoming resistance to β-lactam antibiotics. *J. Org. Chem. 78*, 4207–4213.

5. Chellat, M. F., Raguž, L. and Riedl, R. (2016). Targeting Antibiotic Resistance. *Angew. Chem. Int. Ed. 55*, 6600–6626.

6. González-Bello, C., Rodríguez, D., Pernas, M., Rodríguez, Á. and Colchón, E. (2019). β-Lactamase Inhibitors To Restore the Efficacy of Antibiotics against Superbugs. *J. Med. Chem. ASAP*, 10.1021/acs.jmedchem.9b01279.

7. Tooke, C. L., Hinchliffe, P., Bragginton, E. C., Colenso, C. K., Hirvonen, V. H. A., Takebayashi, Y. and Spencer, J. (2019). β-Lactamases and β-Lactamase Inhibitors in the 21st Century. *J. Mol. Biol. 431*, 3472–3500.

8. Ehmann, D. E., Jahić, H., Ross, P. L., Gu, R.-F., Hu, J., Kern, G., Walkup, G. K. and Fisher, S. L. (2012). Avibactam is a covalent, reversible, non–β-lactam β-lactamase inhibitor. *Proc. Natl. Acad. Sci. 109*, 11663–11668.

9. Wang, D. Y., Abboud, M. I., Markoulides, M. S., Brem, J. and Schofield, C. J. (2016). The road to avibactam: the first clinically useful non-β-lactam working somewhat like a β-lactam. *Future Med. Chem. 8*, 1063–1084.

10. Hecker, S. J., Reddy, K. R., Totrov, M., Hirst, G. C., Lomovskaya, O., Griffith, D. C., King, P., Tsivkovski, R., Sun, D., Sabet, M., Tarazi, Z., Clifton, M. C., Atkins, K., Raymond, A., Potts, K. T., Abendroth, J., Boyer, S. H., Loutit, J. S., Morgan, E. E., Durso, S. and Dudley, M. N. (2015). Discovery of a cyclic boronic acid β-lactamase inhibitor (RPX7009) with utility vs class A Serine carbapenemases. *J. Med. Chem. 58*, 3682–3692.

11. Hirsch, E. B., Ledesma, K. R., Chang, K.-T., Schwartz, M. S., Motyl, M. R. and Tam, V. H. (2012). In vitro activity of MK-7655, a novel β-lactamase inhibitor, in combination with imipenem against carbapenem-resistant Gram-egativne bacteria. *Antimicrob. Agents Chemother. 56*, 3753–3757.

12. Morinaka, A., Tsutsumi, Y., Yamada, M., Suzuki, K., Watanabe, T., Abe, T., Furuuchi, T., Inamura, S., Sakamaki, Y., Mitsuhashi, N., Ida, T. and Livermore, D. M. (2015). OP0595, a new diazabicyclooctane: mode of action as a serine β-lactamase inhibitor, antibiotic and β-lactam 'enhancer'. *J. Antimicrob. Chemother. 70*, 2779–2786.

13. Livermore, D. M., Mushtaq, S., Warner, M., Vickers, A. and Woodford, N. (2017). In vitro activity of cefepime/zidebactam (WCK 5222) against Gram-negative bacteria. *J. Antimicrob. Chemother. 72*, 1373–1385.

14. Durand-Réville, T. F., Guler, S., Comita-Prevoir, J., Chen, B., Bifulco, N., Huynh, H., Lahiri, S., Shapiro, A. B., McLeod, S. M., Carter, N. M., Moussa, S. H., Velez-Vega, C., Olivier, N. B., McLaughlin, R., Gao, N., Thresher, J., Palmer, T., Andrews, B., Giacobbe, R. A., Newman, J. V., Ehmann, D. E., de Jonge, B., O'Donnell, J., Mueller, J. P., Tommasi, R. A. and Miller, A. A. (2017). ETX2514 is a broad-spectrum β-lactamase inhibitor for the treatment of drug-resistant Gram-negative bacteria including *Acinetobacter baumannii*. *Nat. Microbiol. 2*, 17104.

15. Peilleron, L. and Cariou, K. (2020). Synthetic approaches towards avibactam and other diazabicyclooctane β-lactamase inhibitors. *Org. Biomol. Chem. 18*, 830–844.

16. Linciano, P., Cendron, L., Gianquinto, E., Spyrakis, F. and Tondi, D. (2019). Ten years with New Delhi metallo-β-lactamase-1 (NDM-1): from structural insights to inhibitor design. *ACS Infect. Dis. 5*, 9–34.

17. Tehrani, K. H. M. E. and Martin, N. I. (2017). Thiol-containing metallo-β-lactamase inhibitors resensitize resistant Gram-negative bacteria to meropenem. *ACS Infect. Dis. 3*, 711–717.

18. Klingler, F.-M., Wichelhaus, T. A., Frank, D., Cuesta-Bernal, J., El-Delik, J., Müller, H. F., Sjuts, H., Göttig, S., Koenigs, A., Pos, K. M., Pogoryelov, D. and Proschak, E. (2015). Approved drugs containing thiols as inhibitors of metallo-β-lactamases: strategy to combat multidrug-resistant bacteria. *J. Med. Chem. 58*, 3626–3630.

19. King, A. M., Reid-Yu, S. A., Wang, W., King, D. T., De Pascale, G., Strynadka, N. C., Walsh, T. R., Coombes, B. K. and Wright, G. D. (2014). Aspergillomarasmine A overcomes metallo-β-lactamase antibiotic resistance. *Nature 510*, 503–506.

20. Xiang, Y., Chen, C., Wang, W.-M., Xu, L.-W., Yang, K.-W., Oelschlaeger, P. and He, Y. (2018). Rhodanine as a potent scaffold for the development of broad-spectrum metallo-β-lactamase inhibitors. *ACS Med. Chem. Lett. 9*, 359–364.

21. Brem, J., van Berkel, S. S., Aik, W., Rydzik, A. M., Avison, M. B., Pettinati, I., Umland, K.-D., Kawamura, A., Spencer, J., Claridge, T. D. W., McDonough, M. A. and Schofield, C. J. (2014). Rhodanine hydrolysis leads to potent thioenolate mediated metallo-β-lactamase inhibition. *Nat. Chem. 6*, 1084–1090.

22. Leiris, S., Coelho, A., Castandet, J., Bayet, M., Lozano, C., Bougnon, J., Bousquet, J., Everett, M., Lemonnier, M., Sprynski, N., Zalacain, M., Pallin, T. D., Cramp, M. C., Jennings, N., Raphy, G., Jones, M. W., Pattipati, R., Shankar, B., Sivasubrahmanyam, R., Soodhagani, A. K., Juventhala, R. R., Pottabathini, N., Pothukanuri, S., Benvenuti, M., Pozzi, C., Mangani, S., De Luca, F., Cerboni, G., Docquier, J.-D. and Davies, D. T. (2019). SAR studies leading to the identification of a novel series of metallo-β-lactamase inhibitors for the treatment of carbapenem-resistant enterobacteriaceae infections that display efficacy in an animal infection model. *ACS Infect. Dis. 5*, 131–140.

23. Yu, Z.-J., Liu, S., Zhou, S., Li, H., Yang, F., Yang, L.-L., Wu, Y., Guo, L. and Li, G.-B. (2018). Virtual

target screening reveals rosmarinic acid and salvianolic acid A inhibiting metallo- and serine-β-lactamases. *Bioorg. Med. Chem. Lett. 28*, 1037–1042.

24. Brem, J., Cain, R., Cahill, S., McDonough, M. A., Clifton, I. J., Jiménez-Castellanos, J.-C., Avison, M. B., Spencer, J., Fishwick, C. W. G. and Schofield, C. J. (2016). Structural basis of metallo-β-lactamase, serine-β-lactamase and penicillin-binding protein inhibition by cyclic boronates. *Nat. Commun. 7*, 1–8.

25. Cahill, S. T., Cain, R., Wang, D. Y., Lohans, C. T., Wareham, D. W., Oswin, H. P., Mohammed, J., Spencer, J., Fishwick, C. W. G., McDonough, M. A., Schofield, C. J. and Brem, J. (2017). Cyclic boronates inhibit all classes of β-lactamases. *Antimicrob. Agents Chemother. 61*, e02260-16.

26. Krajnc, A., Brem, J., Hinchliffe, P., Calvopiña, K., Panduwawala, T. D., Lang, P. A., Kamps, J. J. A. G., Tyrrell, J. M., Widlake, E., Saward, B. G., Walsh, T. R., Spencer, J. and Schofield, C. J. (2019). Bicyclic boronate VNRX-5133 inhibits metallo- and serine-β-lactamases. *J. Med. Chem. 62*, 8544–8556.

27. Parkova, A., Lucic, A., Krajnc, A., Brem, J., Calvopina, K., Langley, G., McDonough, M. A., Trapencieris, P. and Schofield, C. J. (2019). Broad spectrum β-lactamase inhibition by a thioether substituted bicyclic boronate. *ACS Infect. Dis. ASAP*, 10.1021/acsinfecdis.9b00330.

28. Wang, Y.-L., Liu, S., Yu, Z.-J., Lei, Y., Huang, M.-Y., Yan, Y.-H., Ma, Q., Zheng, Y., Deng, H., Sun, Y., Wu, C., Yu, Y., Chen, Q., Wang, Z., Wu, Y. and Li, G.-B. (2019). Structure-based development of (1-(3′-mercaptopropanamido)methyl)boronic acid derived broad-spectrum, dual-action inhibitors of metallo- and serine-β-lactamases. *J. Med. Chem. 62*, 7160–7184.

29. Pitts, C. R. and Lectka, T. (2014). Chemical synthesis of β-lactams: asymmetric catalysis and other recent advances. *Chem. Rev. 114*, 7930–7953.

30. Staudinger, H. (1907). Zur Kenntniss der Ketene. Diphenylketen. *Justus Liebigs Ann. Chem. 356*, 51–123.

31. DeKorver, K. A., Li, H., Lohse, A. G., Hayashi, R., Lu, Z., Zhang, Y. and Hsung, R. P. (2010). Ynamides: A modern functional group for the new millennium. *Chem. Rev. 110*, 5064–5106.

32. Evano, G., Coste, A. and Jouvin, K. (2010). Ynamides: Versatile tools in organic synthesis. *Angew. Chem. Int. Ed. 49*, 2840–2859.

33. Lu, P. and Wang, Y. (2012). The thriving chemistry of ketenimines. *Chem. Soc. Rev. 41*, 5687–5705.

34. Dodd, R. H. and Cariou, K. (2018). Ketenimines Generated from Ynamides: Versatile Building Blocks for Nitrogen-Containing Scaffolds. *Chem. – Eur. J. 24*, 2297–2304.

35. Hentz, A., Retailleau, P., Gandon, V., Cariou, K. and Dodd, R. H. (2014). Transition-metal-free tunable chemoselective N-functionalization of indoles with ynamides. *Angew. Chem. Int. Ed. 126*, 8473–8477.

36. Romero, E., Minard, C., Benchekroun, M., Ventre, S., Retailleau, P., Dodd, R. H. and Cariou, K. (2017). Base-Mediated Generation of Ketenimines from Ynamides: Direct Access to Azetidinimines by an Imino-Staudinger Synthesis. *Chem. – Eur. J. 23*, 12991–12994.

37. Van Camp, A., Goossens, D., Moya-Portuguez, M., Marchand-Brynaert, J. and Ghosez, L. (1980). Synthesis of N-(tosyl)azetidin-2-imines. *Tetrahedron Lett. 21*, 3081–3084.

38. Whiting, M. and Fokin, V. V. (2006). Copper-catalyzed reaction cascade: direct conversion of alkynes into N-sulfonylazetidin-2-imines. *Angew. Chem. Int. Ed. 45*, 3157–3161.

39. Bonnin, R. A., Poirel, L., Carattoli, A. and Nordmann, P. (2012). Characterization of an IncFII Plasmid Encoding NDM-1 from Escherichia coli ST131. *PLOS ONE 7*, e34752.

40. Verdonk, M. L., Cole, J. C., Hartshorn, M. J., Murray, C. W. and Taylor, R. D. (2003). Improved protein–ligand docking using GOLD. *Proteins Struct. Funct. Bioinforma. 52*, 609–623.

41. Artimo, P., Jonnalagedda, M., Arnold, K., Baratin, D., Csardi, G., de Castro, E., Duvaud, S., Flegel, V., Fortier, A., Gasteiger, E., Grosdidier, A., Hernandez, C., Ioannidis, V., Kuznetsov, D., Liechti, R., Moretti, S., Mostaguir, K., Redaschi, N., Rossier, G., Xenarios, I. and Stockinger, H. (2012). ExPASy: SIB bioinformatics resource portal. *Nucleic Acids Res. 40*, W597–W603.

42. Groom, C. R. and Allen, F. H. (2014). The Cambridge Structural Database in Retrospect and Prospect. *Angew. Chem. Int. Ed. 53*, 662–671.

43. Pettersen, E. F., Goddard, T. D., Huang, C. C., Couch, G. S., Greenblatt, D. M., Meng, E. C. and Ferrin, T. E. (2004). UCSF Chimera—A visualization system for exploratory research and analysis. *J. Comput. Chem. 25*, 1605–1612.

44. Kim, Y., Cunningham, M. A., Mire, J., Tesar, C., Sacchettini, J. and Joachimiak, A. (2013). NDM-1, the ultimate promiscuous enzyme: substrate recognition and catalytic mechanism. *FASEB J. 27*, 1917–1927.

45. Ke, W., Bethel, C. R., Thomson, J. M., Bonomo, R. A. and van den Akker, F. (2007). Crystal Structure of KPC-2: Insights into Carbapenemase Activity in Class A β-Lactamases. *Biochemistry 46*, 5732–5740.

46. King, D. T., King, A. M., Lal, S. M., Wright, G. D. and Strynadka, N. C. J. (2015). Molecular Mechanism of Avibactam-Mediated β-Lactamase Inhibition. *ACS Infect. Dis. 1*, 175–184.

47. Surpateanu, G. and Iorga, B. I. (2012). Evaluation of docking performance in a blinded virtual screening of fragment-like trypsin inhibitors. *J. Comput. Aided Mol. Des. 26*, 595–601.

48. Colas, C. and Iorga, B. I. (2014). Virtual screening of the SAMPL4 blinded HIV integrase inhibitors dataset. *J. Comput. Aided Mol. Des. 28*, 455–462.

49. Martiny, V. Y., Martz, F., Selwa, E. and Iorga, B. I. (2016). Blind Pose Prediction, Scoring, and Affinity Ranking of the CSAR 2014 Dataset. *J. Chem. Inf. Model. 56*, 996–1003.

50. Selwa, E., Martiny, V. Y. and Iorga, B. I. (2016). Molecular docking performance evaluated on the D3R Grand Challenge 2015 drug-like ligand datasets. *J. Comput. Aided Mol. Des. 30*, 829–839.

51. Selwa, E., Elisée, E., Zavala, A. and Iorga, B. I. (2018). Blinded evaluation of farnesoid X receptor (FXR) ligands binding using molecular docking and free energy calculations. *J. Comput. Aided Mol. Des. 32*, 273–286.

52. Chaput, L., Selwa, E., Elisée, E. and Iorga, B. I. (2019). Blinded evaluation of cathepsin S inhibitors from the D3RGC3 dataset using molecular docking and free energy calculations. *J. Comput. Aided Mol. Des. 33*, 93–103.

53. Elisée, E., Gapsys, V., Mele, N., Chaput, L., Selwa, E., de Groot, B. L. and Iorga, B. I. (2019). Performance evaluation of molecular docking and free energy calculations protocols using the D3R Grand Challenge 4 dataset. *J. Comput. Aided Mol. Des. 33*, 1031–1043.